# Thermo-mechanical modeling of snouts deformation

H. Saint-Raymond, N. Bontems

*The snout is the last element which connects the annealing furnace with the zinc bath on Hot Dip Galvanizing line. The main role of the snout is to prevent oxygen atoms to access and damage the steel surface before entering into the zinc pot. Snout-end deformation is today the main reason of snout end-of-life. It generates air leaks, leading to defects generations as non-coated spots. ArcelorMittal R&D developed 3D thermo-mechanical models of industrial snout-ends. Models take into account the industrial snout lifetime, i.e. the successive heating and cooling phases during the snout emersions and immersions in the zinc pot. Boundary conditions were determined thanks to specific measurements at laboratory and on industrial plant. The model shows that the main origin of the snout deformation are the temperature gradients between immersed and non-immersed parts, and the dilatation generated during the snout immersion. The creeping effect appears to be negligible. During heating phase like during the cooling, strong compressive stresses appears in the snout walls leading to cracks occurrence and buckling of the snout walls. In all cases, the level and mode of deformation depend strongly on the snout design and fixation system of the snout lower part. This model has been used to define and to test the actions (snout design and/or operating procedure modifications) which limit and control the snout deformation and to evaluate their impact.*

**Keywords:**
Hot Dip Coating, Snout, Deformations, Thermo-mechanical modeling, temperature gradients, buckling, cracks

## INTRODUCTION

Deformations are today the main reason of snout end-of-life. Snout deformation causes difficulties of air tightness at the junction with the snout upper parts, generating bare spots and/or zinc dust defects[1]. In 2008 & 2009, the frequent stoppage of the galvanizing lines leaded to frequent immersion & emersion of the snout end out of the zinc pot, resulting in a crisis of snout deformations.

## THERMO-MECHANICAL MODELING OF SNOUT DEFORMATIONS

To ensure the best predictability of the results, the first part of this study consisted in collecting the snout drawings of various industrial lines of the ArcelorMittal group. From these drawings, an accurate 3D modeling has been performed. The whole snout is modeled, starting from the flange which is bolted or welded to the furnace casing, up to the snout-end immersed inside the zinc bath. An example of 3D snout model is displayed in Fig. 2. The grey part, so-called the “upper part”, is connected to the furnace casing. The green part, so called the “lower part” or “snout-end”, is immersed inside the zinc bath on one side, and connected to the upper part of the other side. The insulation of the snout upper part is not displayed but was taken into account through the thermal boundary conditions.
The different snout parts are assembled between them by me-

**Hubert Saint-Raymond, Nicolas Bontems**
ArcelorMittal Maizières Research,
Voie romaine BP 30320, F-57283 Maizières-lès-Metz Cedex 01, France

*Paper presented at the 8th Int. Conf. GALVATECH 2011, Genova, 21-25 June 2011, organized by AIM*

**FIG. 1** ***Though their robustness, deformation observed on snout could exceed 80 mm of amplitude.***
*Nonostante la loro robustezza, la deformazione osservabile sugli snout può essere superiore a 80 mm di ampiezza.*

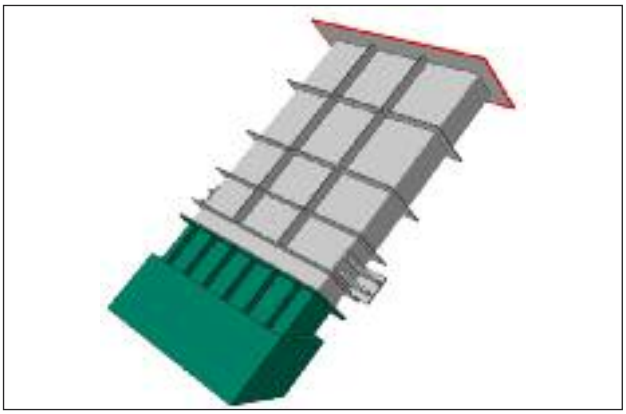

**FIG. 2** ***Snout-ends were modeled in 3D according to the industrial configurations.***
*E’ stato creato un modello 3D delle estremità dello snout secondo le loro configurazioni industriali.*

chanical boundary conditions (bolts, pivot, concentrated forces...) according to the industrial configurations and mechanical systems used to position the snout (weld, hydraulic jacks, simple support,...). In the present case, snout lower and upper parts are welded together and a joint condition was applied to nodes along the weld seam. The snout weight and the pressure applied by the liquid zinc are taken into account.

**Thermal boundary conditions**

Two main parts must be distinguished in terms of boundaries conditions: the part immersed in the zinc bath (the surface has the same temperature as the bath which is about 460°C for GI coating) and the part outside the zinc pot where the walls undergo the three modes of heat transfer: conduction, free and forced convection, and radiation:

a) Conduction: within medium.
b) Convection: inside and outside the snout.
c) Radiation: between steel strip and the internal walls of the snout.

Simulation takes into account the industrial snout life, i.e. the succession of thermal cycles with a heating phase corresponding to the snout immersion into the zinc bath and a cooling phase during the snout emersion out of the zinc pot. To investigate the behavior of the whole snout during these transient phases, we simulate using the model up to 20 successive immersions and emersions of the snout-end in/out of the zinc pot. Immersion of the snout into the zinc bath occurs generally by steps. Fig. 3 presents a case of immersion where the snout is immersed by steps of 10cm every 30 minutes. The complete immersion takes 3 hours and half.

Removing of the snout-end out of the zinc bath is a faster operation. In this case, the whole snout cools down at ambient air with natural convection conditions.

Thermal boundary conditions during immersion (heat fluxes, convection coefficients) have been fitted from thermal measurements done on HDG lines using contact thermocouples and infrared camera, as described by J. Rotole et al[2]. To simulate the cooling of the outer snout walls at ambient temperature, a free convection at room temperature of 30°C is applied to the external walls.

**Rheology of stainless steel at high temperature**

The snout is commonly manufactured of stainless steel, as AISI 304 or 316L steel grades. For the modeling, we needed material's mechanical data covering the whole range of temperature and deformation rate undergone by the snout during transient and working conditions. The literature proposes rheology at room temperature, as the law given by J. Lemaitre and J.L. Chaboche[3] for 316L stainless steel:

$$\sigma = K.\varepsilon^{(p)m}.\dot{\varepsilon}^{(p)n} \quad with \quad \begin{matrix} K = 458 \\ m = -0.0714 \\ n = 0.01538 \end{matrix} \qquad (1)$$

where $\sigma$ is the uniaxial inelastic stress in MPa, m the work hardening coefficient and n the sensitivity coefficient to the deformation rate. However, we had to complete the mechanical data of above mentioned stainless steels for the temperature range and the deformation rate range representative of Hot Dip Galvanizing conditions.

Therefore tensile trials on stainless steel grades were performed. We investigated various temperature (200, 400, 600 °C) and various deformation rate ($10^{-2}$, $10^{-4}$, $10^{-6}$ $s^{-1}$). Fig. 4 shows the behavior of stainless steel 316L for two temperature levels.

The measured rheological curves were directly input in the model, without making any parameter identifications. For the intermediate temperature, a linear interpolation of rheological laws is made based on the measured curves.

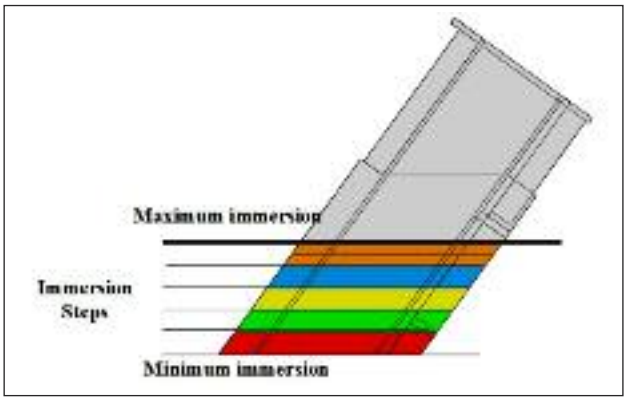


**FIG. 3** ***Immersion by step of 10cm each ½ hour.***

*Immersione con passaggi di 10 cm ogni mezz'ora.*

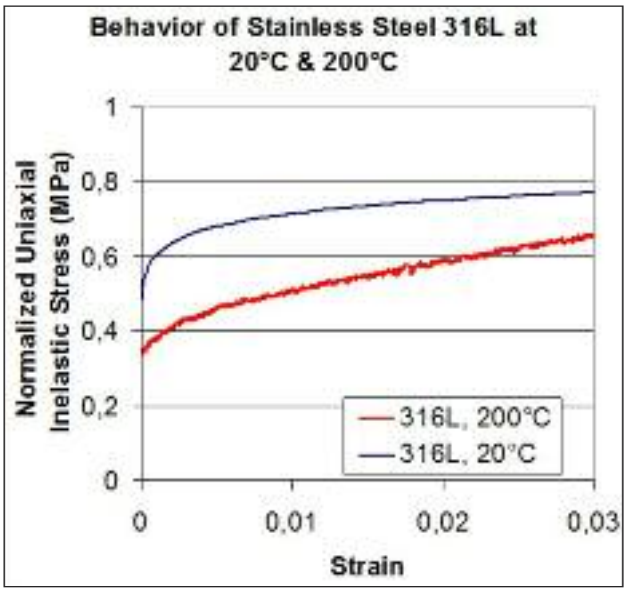


**FIG. 4** ***Experimental rheological measurements supply the mechanical laws used by the model.***

*Le misurazioni reologiche sperimentali forniscono le leggi meccaniche utilizzate dal modello.*

Simulations were performed on various industrial snouts of the ArcelorMittal group. Two main studies were performed:

- In a first step, the influence of the snout design for a given boundary conditions set;
- In a second attempt, the influence of process parameters on the snout behavior.

RESULTS

**Validation**

To insure the highest predictability, the model takes into account the main parameters characterizing the snout life: 3D design and mechanical boundary conditions, measured rheologies & thermal conditions, succession of immersion/emersion operations. As a result: a good agreement between simulated and observed snout deformations is obtained. Figure 5 compares the shape of the snout-end after fives immersion in simulation to the reality. Both industrial snout and modeled snout have the same deformation pattern: a strong bulging of the snout-end

**FIG. 5**
***Bulging of the snout-end rear side is well reproduced by the model.***
*La bombatura della parte posteriore dell'estremità dello snout è ben riprodotta dal modello.*

**FIG. 6**
***The temperature of the snout is not homogeneous and varies strongly with the time.***
*La temperature dello snout non è omogenea e varia fortemente nel tempo.*

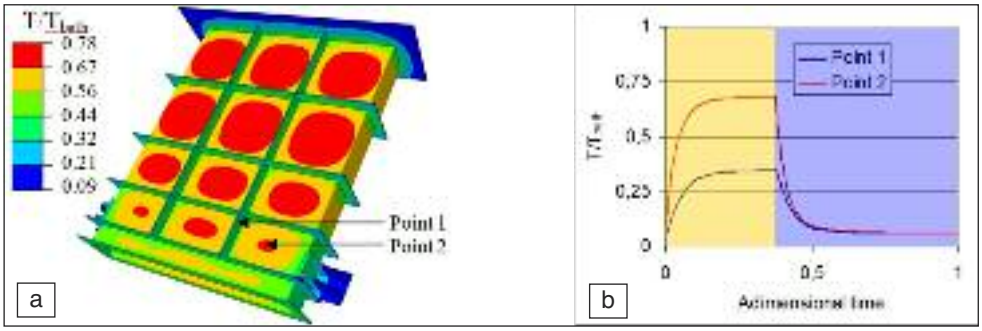


**FIG. 7**
***Displacement of the broad faces according to U1.***
*Dislocamento delle pareti larghe secondo U1.*

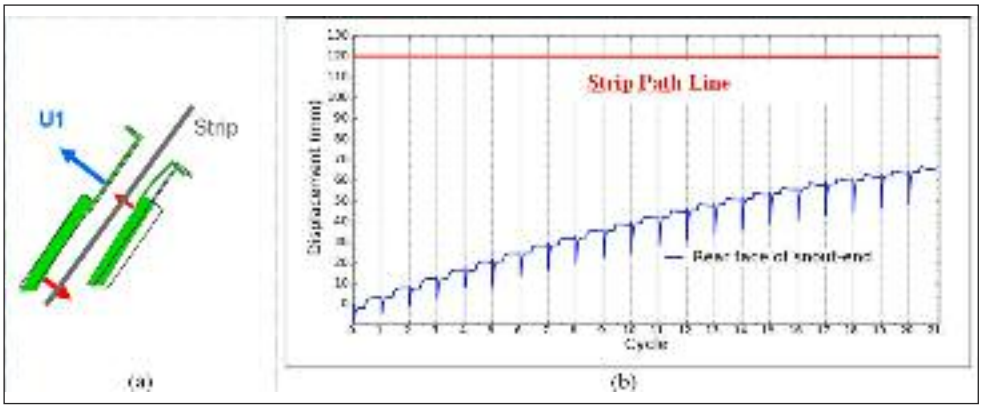


front face, strong displacements of the snout rear side, and a subsequent deformation of the flange.

**Thermal behavior**

Fig. 6(a) and (b) display respectively, the distribution of temperature at the snout surface once the thermal steady state is reached (corresponding to production conditions) and the evolution of the temperature at the snout surface during immersion and emersion phases. From Fig. 6 a), it is clear that the presence of stiffeners at the surface of the snout increases locally the cooling by surface increase and therefore creates strong temperature variations at snout inner and outer surfaces.
More over, Fig. 6 b) indicates also that the temperature of snout walls evolves much with the time due to the thermal conduction from the zinc pot and due to the radiation coming from the strip. As a consequence, strong thermal gradients appear in the snout walls, and these thermal gradients evolve with the times.

**Increasing snout deformations**

One major consequence of the evolution of the thermal gradient is a cycling of the deformation pattern. Fig. 7 presents the profile of the snout-end in cold state (definitive deformation) after 20 immersion/emersion operations (in green) compared to the initial design (in grey). It displays clearly how the rear side of the snout-end bulges and moves toward the strip. As a consequence, the space dedicated to the strip path line is strongly reduced. In the worse cases, the rear side moves up to touching the strip and making subsequent strip scratches. Fig. 7 b) highlights the displacement evolution of the rear side center along the axis u1 (perpendicular to strip), cycle by cycle. We can see that the deformation increases after each cycle of about 3 to 4 mm, reaching a total displacement of 70 mm after 20 cycles. As a consequence, the distance between the strip and the snout wall (strip path line) is reduced from 120 mm to only 50 mm in only 20 cycles. And deformations would keep on increasing if the number of cycles is still rising. The observed link between the snout deformations and the HDG line stoppage frequency is confirmed.
Deformation of the broad snout walls and reduction of the strip path line are not the only problems generated by the thermal fluctuations. The deformations and displacements of the snout lower part are mechanically transmitted throughout the whole snout, up to the connecting flange welded to the furnace casing. As a consequence, the flanges are also submitted to strong deformations. Fig. 8 compares the flange profile (connection between snout lower and upper part) at the initial state and after 20 immersions/emersions in/out of the zinc bath.
The center of the rear flange moves of about 10 mm away from its initial position due to the overall deformation of the snout. Additionally, the flange bulges also with a maximum displace-

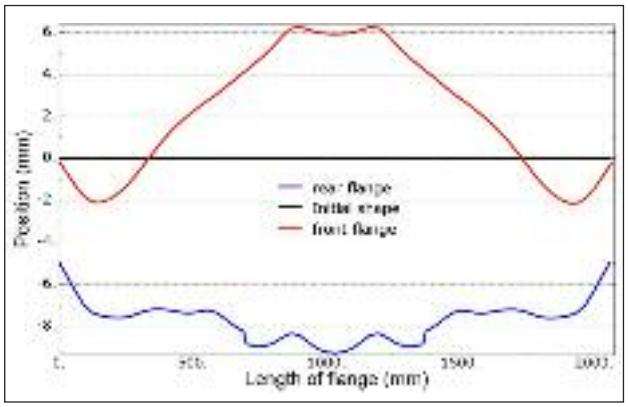


**FIG. 8** ***Deformations of the flange at the junction between snout lower and upper parts might generate air tightness difficulties.***

*Deformazioni della flangia in prossimità della giunzione fra le parti inferiore e superiore dello snout potrebbero creare difficoltà nella tenuta d'aria.*

ment of about 5 mm for the rear side, 8 mm for the front side, between the corner and the center. Such big deformations are plastic and remain even after demounting of the snout. As a consequence, the air tightness of the junction between the snout-end and the upper snout part can be strongly disturbed. It makes also the replacement of the snout-end quite tricky.

### Cracking

Besides the deformation of the snout which can lead to quality and maintenance difficulties, deformations might also lead to cracking of the snout. Fig. 9 and Fig. 10 show a typical case of stresses and strain concentration area generated by the successive thermal cycles. In Fig. 9, it can be seen that strong deformations develop in the vicinity of the connection with the furnace casing, reaching values above 10% after 20 cycles.
Fig. 10 highlights that all these deformations and stresses are generated during the cooling stage. Efforts field is mainly composed of uniaxial stresses, with the transversal direction being particularly solicited. It underlines that the stiff "welded" connection between the snout and the furnace does not allow enough flexibility to absorb the thermal distortion. In accordance with the uniaxial stresses, high shear stresses develop also in the corner, reaching almost 200 MPa.

### Buckling of the snout walls under the thermal gradients

The results presented above explain the physical phenomena that are industrially observed on the galvanizing snouts. It highlighted an evolution of the whole snout deformation with the time, linked with the successive immersion/emersion cycles. In the worse cases it leads to crack opening.
Fig. 11 shows, at a point located in the middle of the snout-end broad face, the evolution with the time of the temperature and the average stresses. It highlights that the snout-end front broad face is firstly in traction due to the thermal gradients and the first distortions occurring in the already immersed parts. Then, when the temperature at the investigated point starts to increase, the tension stresses turns to very high compressive stresses
The compression stress reaches 80MPa (Fig. 11), which is, considering the snout geometry, high enough to create a buckling of the snout wall. The snout walls buckling leads to the observed deformations and cracks. The compression stresses result mainly from the dilatation of the snout walls and from a lack of freedom in the whole system. The buckling deformation mode is defined by the snout geometry associated with the strong thermal gradients existing across the snout wall thickness, above the zinc free surface. Buckling initiates when the buckling critical stress which is characteristic to the snout design, is exceeded.

**FIG. 9**
***Cracks appear at the tip of the flange.***

*Cricche si generano all'estremità della flangia.*

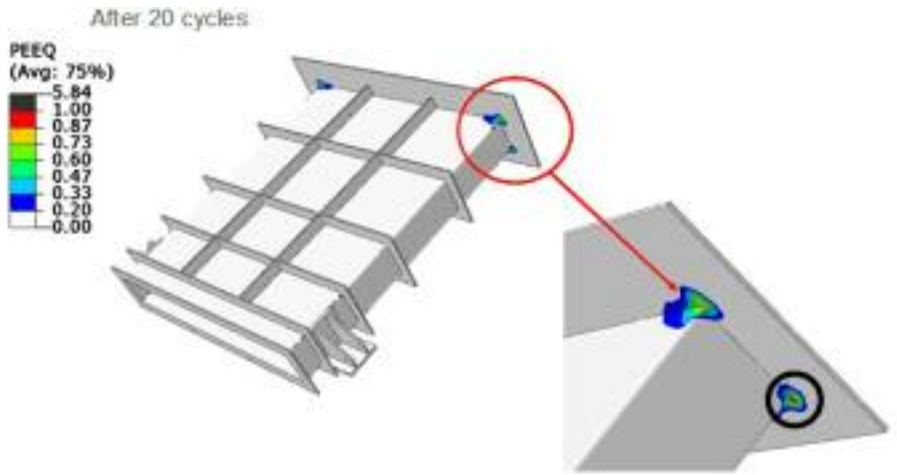


**FIG. 10**
***Strong shear stresses appear in the vicinity of the connecting flange when snout end returns to cold state.***

*Forti tensioni di taglio si sviluppano presso la flangia di connessione quando l'estremità dello snout ritorna allo stato freddo.*

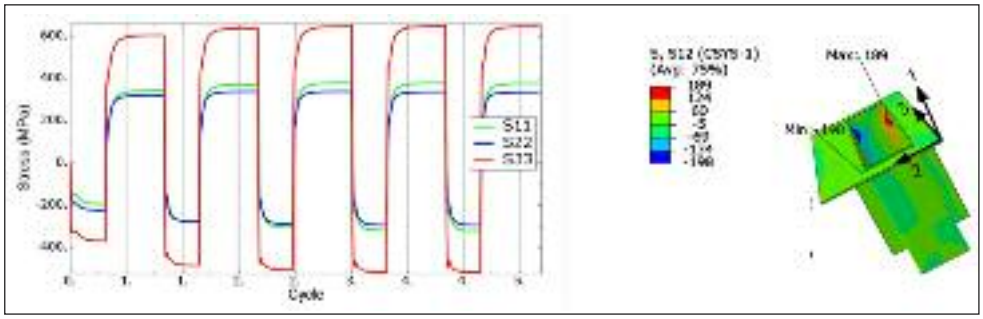

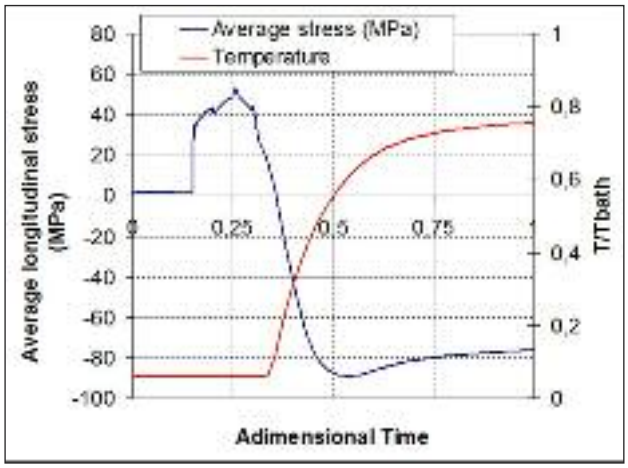


**FIG. 11** ***Compression stresses appearing in the snout wall during the heating phase generate snout wall buckling phenomenon.***

*Le tensioni di compressione che si sviluppano nella parete dello snout durante la fase di riscaldo generano fenomeni di instabilità a carico di punta nella parete dello snout.*

CONCLUSIONS - PERSPECTIVES

The model shows that the main origin of the snout deformation are the temperature gradients between immersed and non-immersed parts, and the dilatation generated during the snout immersion. The creeping effect appears to be negligible. During heating phase like during the cooling, strong compressive stresses appear in the snout walls leading to cracks occurrence and snout walls buckling. In all cases, the level and mode of deformation depend strongly on the snout design and fixation system of the snout lower part. This model has been used to define and test the actions (snout design and/or operating procedure modifications) which limit and control the snout deformation and to evaluate their impact.

REFERENCES

[1] H. SAINT-RAYMOND, D. BETTINGER, P. OSMONT and J-C DENQUIN "Coating Quality Improvement of Hot Rolled Galvanized Products" Proceedings of Galvatech'07, Osaka, Japan, November 19-22, (2007), pp. 279-284

[2] J. ROTOLE, V. KRISHNARDUL and C. SHASTRY, "Thermal Gradient Characterization of the Snout on a Hot Dip Galvanizing Line," Proc. of AISTech 2008. Iron & Steel Technology Conf, (2008), vol 2 pp. 569-578.

[3] J. LEMAITRE and J.L. CHABOCHE" Mécanique des Matériaux Solides", 2009, Dunod, Paris

## Abstract

### Modellazione termo-meccanica della deformazione degli snout

**Parole chiave:** modellazione - rivestimenti

Lo snout è l'ultimo elemento che collega il forno di ricottura con il bagno di zinco sulla linea di zincatura per immersione a caldo. Il ruolo principale dello snout è quello di impedire l' accesso agli atomi di ossigeno e di danneggiare la superficie dell' acciaio prima di entrare nel bagno di zinco. La deformazione dell'estremità dello snout oggi rappresenta il motivo principale del fine vita dello snout.Questa provoca infiltrazioni d'aria, e porta alla formazione di difetti come chiazze non rivestite. ArcelorMittal R & D ha sviluppato modelli termo-meccanici 3D delle estremità degli snout industriali. Questi modelli tengono conto della durata industriale dello snout, cioè le successive fasi di riscaldamento e di raffreddamento durante le immersioni e le emersioni dello snout nel bagno di zinco. Sono state determinate condizioni limite, grazie a misurazioni specifiche in laboratorio e su impianti industriali. Il modello mostra che l'origine principale della deformazione dello snout sono i gradienti di temperatura tra le parti immerse e quelle non immerse e la dilatazione generata durante l'immersione dello snout.
L'effetto di creep sembra essere trascurabile. Sia durante la fase di riscaldamento che durante il raffreddamento, si generano forti sollecitazioni di compressione nelle pareti dello snout che portano alla comparsa di cricche e alla deformazione delle pareti dello snot. In tutti i casi, il livello e la modalità di deformazione dipendono fortemente dalla forma dello snout e dal sistema di fissaggio della parte inferiore dello stesso. Il modello presentato è stato utilizzato per definire e per sottoporre a prova le azioni (progettazione dello snout e / o modifiche alla procedura di funzionamento) che limitano e controllano la deformazione dello snout e per valutarne l'impatto.